CCFE
CULHAM CENTRE FOR FUSION ENERGY

UK Atomic Energy Authority

UKAEA-CCFE-PR(22)14

R O Dendy, B Chapman-Oplopoiou, B C G Reman, J W S Cook

A new mechanism for collective energy transfer from neutral beam-injected ions to fusion-born alpha-particles on cyclotron timescales in a plasma

A new mechanism for collective energy transfer from neutral beam-injected ions to fusion-born alpha-particles on cyclotron timescales in a plasma

R O Dendy, B Chapman-Oplopoiou, B C G Reman, J W S Cook

This is a preprint of a paper submitted for publication in
Physical Review Letters

A new mechanism for collective energy transfer from neutral beam-injected ions to fusion-born alpha-particles on cyclotron timescales in a plasma

R. O. Dendy,[1,2] B. Chapman-Oplopoiou,[1] B. C. G. Reman,[3,2] and J. W. S. Cook[1]

[1] *UKAEA-CCFE, Culham Science Centre, Abingdon, OX14 3DB, UK*

[2] *Centre for Fusion, Space and Astrophysics, Department of Physics, Warwick University, Coventry CV4 7AL, UK*

[3] *Laboratoire Plasma et Conversion d'Energie, Université Toulouse 3, F-31062 Toulouse, France*

(Dated: January 19, 2022)

Helium ash alpha-particles at $\sim$ 100keV in magnetically confined fusion plasmas may have the same Larmor radius, as well as cyclotron frequency, as the energetic beam-injected deuterons that heat the plasma. While the velocity-space distribution of the helium ash is monotonically decreasing, that of the energetic deuterons is a delta-function in the edge plasma. Here we identify, by means of first principles particle-in-cell computations, a new physical process by which Larmor radius matching enables collective gyroresonant energy transfer between these two co-located minority energetic ion populations, embedded in majority thermal plasma. This newly identified phenomenon rests on similar underlying physics to widely observed ion cyclotron emission from suprathermal minority ion populations.

Future magnetically confined fusion (MCF) plasmas will be sustained at high temperatures $>$ 20keV by collisional heating from alpha-particles born at 3.5MeV in reactions between thermal deuterons and tritons. The lifetime of these plasmas will greatly exceed the slowing-down time of alpha-particles, whose thermalizing distribution in velocity-space will approximate to a monotonically decreasing Lorentzian [1], with characteristic energy of order a few hundred keV. The cool core ($<$ 100keV) of this minority population, comprising alpha-particles which have given up most of their birth energy, is referred to as "Helium ash". The negative slope of the velocity-space distribution implies that electromagnetic waves that enter into wave-particle resonance with the thermalizing alpha-particles may be damped.

A second minority suprathermal ion population is typically created by neutral beam injection (NBI) at energies $\sim$ 100keV, whose primary purpose is usually to heat the thermal ions in the MCF plasma core. Recent studies [2–4] show that collective relaxation of a freshly-ionised subset of the NBI ions, with an initially delta-function velocity distribution in the edge plasma near the injection point, excites the radiation in the ion cyclotron range of frequencies that is observed in the KSTAR tokamak [2] and LHD heliotron-stellarator [3, 4]. This is a form of ion cyclotron emission (ICE), whose power spectrum typically exhibits several strongly suprathermal peaks at low integer harmonics of the cyclotron frequency of the injected ions. ICE is widely observed from MCF plasmas. In addition to historical observations from the TFR [5] and JET [6, 7] tokamaks, and from deuterium-tritium plasmas in JET [8, 9] and TFTR [10], ICE has recently been reported and analysed from the KSTAR [2, 11–13], JT-60U [14, 15], DIII-D [16, 17], ASDEX-Upgrade [18–21], TUMAN-3M [22, 23], NSTX-U [24, 25] and EAST [26] and JET [27] tokamaks, and from LHD [3, 4, 28, 29]. ICE is under consideration as a fast-ion diagnostic for ITER [30–32]; it is also observed from solar-terrestrial plasmas [33–37], and may be present downstream of supernova remnant shocks [38].

ICE is driven by the magnetoacoustic cyclotron instability (MCI) [2, 4, 8–13, 17–21, 33–35, 38–52], which arises when a strongly non-Maxwellian minority energetic ion population enters cyclotron resonance with a fast Alfvén wave propagating nearly perpendicular to the local magnetic field. This resonance can either be wave-wave [40–42], between cyclotron harmonic waves supported by the minority ions and fast Alfvén waves supported by the bulk plasma, or wave-particle [44, 45], at Doppler-shifted cyclotron resonance between the minority ions and the Alfvén wave. To strongly excite the MCI, the local distribution of ions in velocity-space must have a positive gradient with respect to the velocity component perpendicular to the magnetic field, $v_\perp$, in the region of velocity space where $v_\perp \sim v_A$, where v_A is the local value of the Alfvén velocity [4, 40, 41, 44, 45].

Particularly relevant to the present study is the observed ICE that is driven by collective relaxation of NBI ions under the MCI, which has been simulated [2–4, 17] from first principles using particle-in-cell (PIC)-based kinetic codes, notably EPOCH [53]. These solve the Maxwell-Lorentz system of equations self-consistently for tens of millions of gyro-orbit-resolved particles, thus capturing the full physics of cyclotron resonance. In both analytical and computational studies, the initial velocity-space distribution of the ICE-relevant NBI ions is approximated by a ring-beam delta-function with argument $v_\perp \sim v_{NBI}$, where v_{NBI} corresponds to their injection energy. The thermal majority and energetic NBI ions are often of the same species. For example, the NBI ions are sub-Alfvénic deuterons at 80keV to 100keV in KSTAR deuterium plasmas [2], super-Alfvénic and sub-Alfvénic protons at 40keV in LHD hydrogen plasmas [3], and sub-Alfvénic deuterons at 70keV in LHD deuterium plasmas [4].

In the edge region of a deuterium-tritium MCF plasma undergoing nuclear burning there may therefore coexist two energetic minority ion populations - thermalizing alpha-particles, and freshly ionised NBI ions - in addition to the thermal majority ions. The constituent ions in these two minority populations will have comparable cyclotron frequencies and Larmor radii. For example, at the same location in space, there may exist an NBI deuteron and a Helium ash alpha-particle which gyrate about the local magnetic field line with the same frequency and Larmor radius. The velocity-space distributions from which these two ions are drawn will be radically different: a monotonic decrease for the alpha-particles, implying damping of waves at cyclotron resonance; and an MCI-driving delta-function for the NBI ions. These considerations point to an intriguing and potentially important new plasma physics phenomenon, which has not been previously identified, to our knowledge.

We report here a new collective process that can rapidly and directly transfer kinetic energy from NBI deuterons to Helium ash alpha-particles, on cyclotron timescales. Our PIC studies show that the physics involves a generalisation of the MCI. The energy transfer between the two energetic ion populations is mediated by the electric and magnetic fields which are collectively excited by the NBI deuterons, and supported also by the bulk thermal plasma. This process dominates the energy flow of the MCI, in contrast to the related ICE case, where the energy flow is dominated by electromagnetic field excitation on the fast Alfvén-cyclotron harmonic wave branch. Under edge plasma conditions, where the velocity-space distribution of the NBI ions approximates to a ring-beam, this new effect is found to be strongest for a characteristic helium ash temperature 0.1MeV which is comparable to the injection energy of the NBI deuterons. The two energetic ion populations have the same cyclotron frequency, and we find that energy transfer occurs predominantly between deuterons and alpha-particles that have similar Larmor radii, and involves bunching in gyrophase. To our knowledge, this is the first study of direct local collective energy transfer from NBI ions to alpha-particles, on cyclotron timescales, in MCF plasmas. In the demonstration-of-principle simulations reported here, of order ten per cent of the energy of NBI ions that become ionised in the edge region can be transferred to the alpha-particles.

We have run PIC calculations of the Maxwell-Lorentz dynamics of tens of millions of interacting particles, together with their self-consistent electric and magnetic fields, drawn from four populations. Two are thermal: the electrons, and the majority deuterons, with $T_D = 5\text{keV} = T_e$. Two are energetic minorities. First, the minority NBI deuterons with injection energies $E_{NBI} =$ 80keV, 140keV, or 200keV, which are represented by an initial delta-function in perpendicular velocity. Second, the minority alpha-particles, which are represented by a Maxwellian with temperatures $T_{th,\alpha} = 0.1\text{MeV}$, 0.5MeV or 1.0MeV; the lowest of these temperatures is a good approximate model for fully slowed-down Helium ash. Simulation parameters are broadly representative of JET plasmas, with electron number density $n_e = 9.8 \times 10^{19}\text{m}^{-3}$ and magnetic field strength $B_z = 2.7\text{T}$ oriented perpendicular to the 1D3V PIC code spatial domain. It follows that the ratio of NBI ion speed v_{NBI} to local Alfvén speed V_A for the three injection energies is $v_{NBI}/V_A = 0.66$, 0.87 and 1.04 respectively; for alpha-particles at their thermal energy for the three temperatures, the corresponding speed ratio is $v_{Th,\alpha}/V_A = 0.52$, 1.16 and 1.64. The ratios v_{NBI}/V_A and $v_{Th,\alpha}/V_A$ are the key dimensionless parameters governing the physics of the MCI for this model in this regime, and the nine cases examined in Fig.1 and Fig.2 together cover a range of possible values for the fixed local equilibrium density and magnetic field strength. Each PIC simulation uses 10150 grid cells with 1000 particles per cell. In most cases, the ratio of alpha-particles to thermal deuterons $\xi_\alpha = 10^{-3}$, and the ratio of NBI deuterons to thermal deuterons $\xi_{NBI} = 10^{-3}$. Insofar as these values may be unphysically high, this is necessary to enable the physics to unfold in our PIC simulations using acceptable computational resources. Precedents from previous ICE studies [49–51] suggest that the phenomenology is scalable with respect to the concentration of energetic ions.

The multi-species plasma, initialised as above, relaxes,

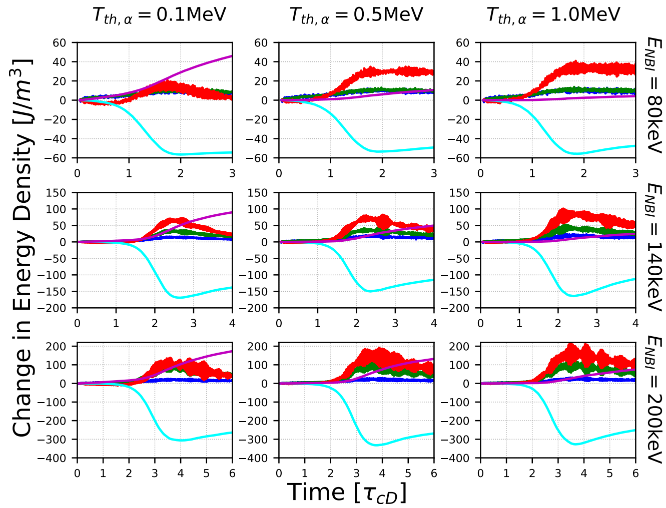

FIG. 1. (color online). Time evolution of the change in energy density of particles and electric and magnetic fields in multiple PIC simulations with initial NBI deuteron energies 80keV, 140keV, and 200keV (rows from top to bottom), and initial helium ash temperatures 0.1MeV, 0.5MeV, and 1.0MeV (columns from left to right). Time is normalised to the deuteron gyroperiod τ_{cD}. The traces, their peaks ordered from top to bottom in the upper left panel, are: Top (magenta) the change in kinetic energy density of the minority alpha-particles; Second (red) the change in kinetic energy density of the thermal bulk plasma deuterons; Third (green) the energy density of the magnetic field perturbation ΔB_z; Fourth (blue) the energy density of the electrostatic field E_x; Fifth (cyan) the change in kinetic energy density of the minority energetic NBI deuterons.

and the time evolution of particle and field energy densities is shown in Fig.1 for nine representative cases. The right-hand column of Fig.1 shows baseline ICE-type phenomenology for the relaxation of NBI ions under the MCI, as seen in, for example, Fig.4 of Ref.[2] and of Ref.[3]. This is dominated by energy transfer from the NBI deuterons to the excited fast Alfvén waves, whereas energy transfer involving the alpha-particles is relatively insignificant. The Alfvén waves incorporate the kinetic energy of coherent oscillations of the thermal deuterons, in addition to electric and magnetic fields. Our newly identified effect appears in the left-hand column of Fig. 1: after an initial ICE-type phase, in the nonlinear regime the dominant long-term energy transfer is from the minority energetic NBI deuterons to the minority energetic alpha-particle population. About ten per cent of the total NBI deuteron kinetic energy is lost; the majority of this is transferred to the alpha-particles in the cases in the left column of Fig. 1, and these proportions are invariant with respect to ξ_α.

Figure 2 plots snapshots of the distribution in perpendicular velocity-space of the alpha-particles: initially Maxwellian with $T_{th,\alpha} = 0.1$MeV at $t = 0$ (upper row); and output from our PIC simulations at $t = 5\tau_{cD}$ (lower row). The three columns are for the cases of NBI deuterons, initially distributed as a ring-beam delta-function in perpendicular velocity, with energies 80keV, 140keV and 200keV. In each panel the alpha-particle velocity is normalised to the NBI deuteron velocity for that case. It is evident from Fig.2 that the energy flows primarily from the NBI deuterons to alpha-particles that have the same perpendicular velocity, causing a plateau around $v_{\perp\alpha} \sim v_{\perp NBI}$. Recalling that the deuterons and alpha-particles have the same cyclotron frequency, it follows that the energy transfer is between ions that have closely similar Larmor radii. This implies that cyclotron resonance is central to the physics of the newly identified energy transfer process.

Gyrobunching in velocity space is therefore expected, and is evident in Fig.3. This is a snapshot at $t = 2\tau_{cD}$ of the distribution of NBI deuterons with respect to the spatial domain x and gyroangle α, for the 1D3V PIC simulation considered in the central panel of Fig.1. The S-shaped striations in Fig.3 are characteristic of cyclotron resonant ion gyrobunching; see, for example, Fig.3 of Ref.[54] and Fig.4 of Ref.[49], and references therein.

In Fig.3, the x-axis units are constructed by normalising position to V_A/Ω_D, where Ω_D is the deuteron angular cyclotron frequency. This normalisation factor has units of metres per radian, which is the inverse of the units used in Fig.4 for wavenumber. The range of the x-domain is from zero to 2π metres per radian; this facilitates direct conversion from the number of striations counted in Fig.3 to wavenumber as considered in Fig.4, which plots the spatiotemporal Fourier transform of the excited B_z magnetic field component in our simulation. Visual inspection of Fig.3 indicates that there are 43 striations in the interval from zero to 2π. This implies a wave-

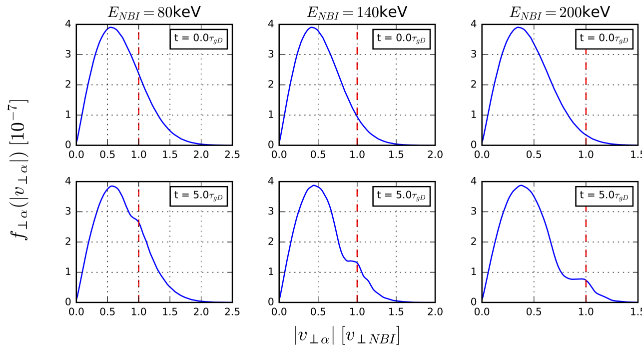

FIG. 2. (color online). Snapshots of the distribution in perpendicular velocity-space of the alpha-particles (blue): initially Maxwellian with $T_{th,\alpha} = 0.1$MeV at $t = 0$ (upper row); and output from our PIC simulations at $t = 5\tau_{cD}$ (lower row). The three columns are for the cases of NBI deuterons, initially distributed as a ring-beam delta-function in perpendicular velocity, with energies 80keV, 140keV and 200keV. In each panel the alpha-particle velocity is normalised to the NBI deuteron velocity for that case. The vertical dashed line (red) denotes where the Larmor radius of alpha-particles equals that of NBI deuterons.

length in these units of $\lambda = 2\pi/43[V_A/\Omega_D]$ and hence a wavenumber $k = 2\pi/\lambda = 43[\Omega_D/V_A]$. This value can be seen to align with the dominant wavenumber structure in Fig.4. This field mediates the interaction between deuterons and alpha-particles. It is evident from Fig.4 that its dominant cyclotron harmonic components lie in the range between thirtieth and fortieth, on the fast Alfvén wave branch which extends diagonally from the origin. Quasi-horizontal low integer cyclotron harmonic waves are visible, here populated by noise through the fluctuation-dissipation theorem [55]. Their intersection with the fast Alfvén branch is the locus of strong MCI drive in edge ICE scenarios; much higher cyclotron harmonics dominate in the scenario considered here, see also the inset of Fig.4.

The two panels of Fig.5 compare the power spectra of fields excited in otherwise identical simulations with different concentrations (one negligible) of minority alpha-particles with $T_{th,\alpha} = 0.1$MeV. These spectra are obtained from PIC-hybrid simulations (that is, with fluidised electrons; see Ref.[2]) for NBI deuterons at 140 keV in a deuterium thermal plasma. Each ion species is represented with 400 particles per cell, and the simulation domain has 1024 cells. The spectra result from Fourier transforming the self-consistent fields that are excited in the simulations, summing over a time interval $10\tau_{cD}$. In both cases, the excited (above noise) field energy is bunched with spectral peaks in the two groups of cyclotron harmonics already identified from the full PIC simulation in Fig.4, around the thirtieth and the thirty-fifth. The primary difference is the diminished field energy around the 35th cyclotron harmonic in the upper panel. This reflects energy which has flowed from the

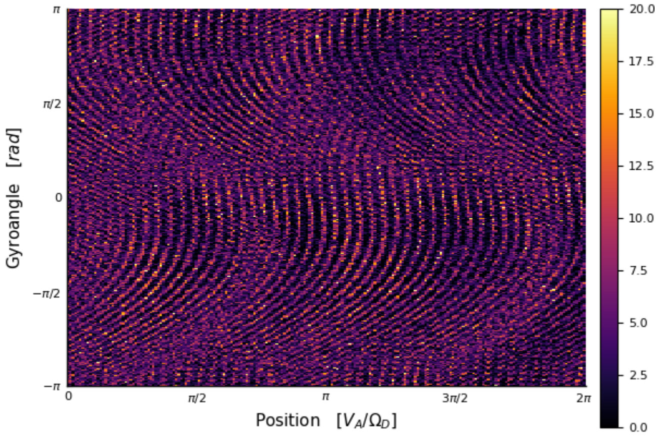

FIG. 3. (color online). Gyrobunching: a snapshot of the distribution of NBI deuterons, initially at 140keV, with respect to the spatial domain x and gyroangle α, from a 1D3V PIC simulation for a thermal deuterium plasma ($T_D = 5$keV) which also contains a minority alpha-particle population with temperature $T_{th,\alpha} = 1$ MeV. The choice of normalisation facilitates comparison with Fig.4, see main text.

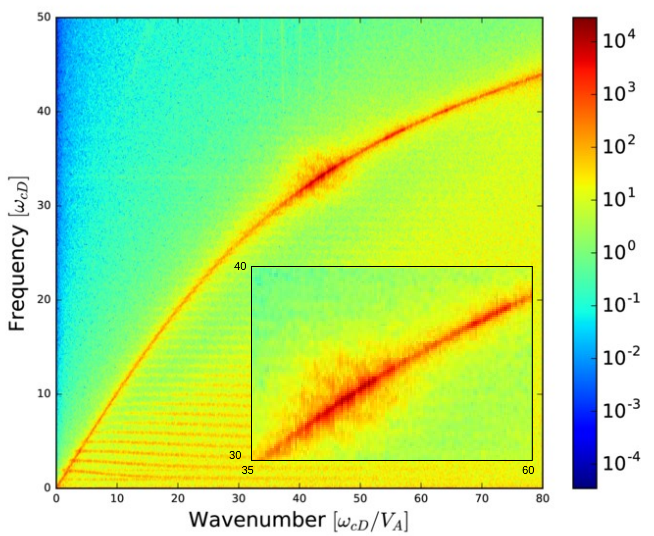

FIG. 4. (color online). Spatiotemporal Fourier transform of the excited z-component of the magnetic field in a PIC simulation with Field energy is concentrated between the thirtieth and fortieth cyclotron harmonics, on the fast Alfvén wave branch. Inset: an expanded plot of the region between the 30th and 40th cyclotron harmonics.

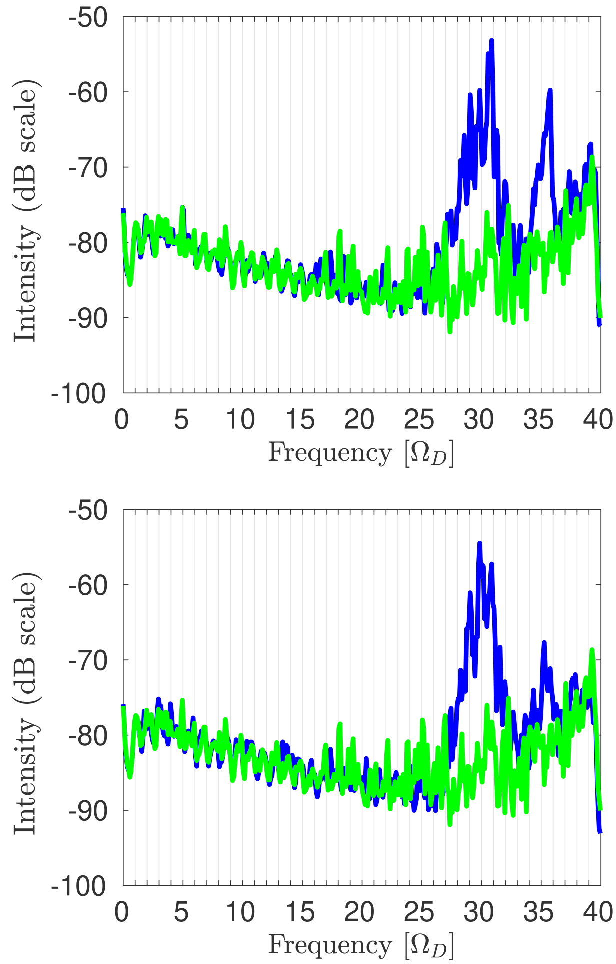

FIG. 5. (color online). Frequency power spectra (blue) obtained from the spatiotemporal Fourier transform of excited fields in PIC-based simulations at $t = 10\tau_{cD}$. In both cases NBI deuteron concentration $\xi_{NBI} = 10^{-3}$. The lower panel is for negligible alpha-particle concentration $\xi_\alpha = 10^{-6}$, hence a pure ICE scenario. The top panel is for $\xi_\alpha = 10^{-3}$, the scenario of Figs.1 and 2. Green traces are the fluctuation-dissipation noise baseline. Frequency is in units of the deuteron (equivalently alpha-particle) gyrofrequency. The primary difference between these excited spectra is around the 35th deuteron cyclotron harmonic.

NBI deuterons to the alpha-particles in the Helium ash case of $\xi_\alpha = 10^{-3}$, instead of flowing to the excited fields in the ICE-type case of $\xi_\alpha = 10^{-6}$.

We have identified a new collective cyclotron resonant process that can shift energy rapidly from freshly injected NBI deuterons to thermalizing fusion-born alpha-particles, in a majority thermal plasma where both energetic ion species are present. The energy transfer is concentrated between the subset of ions of both species that have similar Larmor radii. For the MCF edge plasma scenario considered here, this selection criterion is effectively governed by the component of the injection energy of the NBI deuterons that is perpendicular to the magnetic field. The physics of energy transfer is a generalisation of the MCI, the instability which underlies observations of ICE from MCF plasmas in general and, in particular, from NBI ion populations in the edge plasmas of the KSTAR tokamak and the LHD heliotron-stellarator. This newly identified effect is also likely to be strongest in edge plasmas, where the freshly ionised NBI ions approximate to a ring-beam in velocity space, and energy transfer is to helium ash alpha-particles with comparable energies ~ 0.1MeV. In the locally uniform demonstration-of-principle simulations presented here, the maximum proportion of NBI deuteron energy lost is of order ten per cent. It therefore appears possible that noticeable diminution of NBI power delivered to the core plasma could occur by this new process, under conditions where alpha-particle production in fusion reactions is substantial. The present results extend the reach of the MCI in MCF plasma physics, where it has also been identified as a potential mechanism for alpha channelling [56] as well as the driving mechanism for ICE. There may also be consequences, for future investigation, for the confinement and transport of Helium ash in the edge plasma. Experimental testing of the present theory could perhaps be carried out using minority energetic Helium ion populations generated, as in Ref.[57], using a three-ion cyclotron resonant heating scenario [58, 59]. It is helpful that this approach, like classic minority ion cyclotron resonant heating scenarios (for which see, for example, Fig.5 of Ref.[60]), predominantly raises the perpendicular energy component of the heated ions, and hence their Larmor radii.

This work received support from the RCUK Energy Programme grant no. EP/T012250/1. It was carried out within the framework of the EUROfusion Consortium and has received funding from the Euratom research and training programme 2014-2018 and 2019-2020 under grant agreement No 633053. The views and opinions expressed herein do not necessarily reflect those of the European Commission.

[1] D. Spong, D. Sigmar, K. Tsang, J. Ramos, D. Hastings, and W. Cooper, Physica Scripta **1987**, 18 (1987).
[2] B. Chapman, R. Dendy, S. Chapman, K. McClements, G. Yun, S. Thatipamula, and M. Kim, Nuclear Fusion **59**, 106021 (2019).
[3] B. Reman, R. Dendy, T. Akiyama, S. Chapman, J. Cook, H. Igami, S. Inagaki, K. Saito, and G. Yun, Nuclear Fusion **59**, 096013 (2019).
[4] B. Reman, R. Dendy, T. Akiyama, S. Chapman, J. Cook, H. Igami, S. Inagaki, K. Saito, R. Seki, M. Kim, *et al.*, Nuclear Fusion **61**, 066023 (2021).
[5] T. Equipe, Nuclear Fusion **18**, 1271 (1978).
[6] G. Cottrell and R. Dendy, Physical Review Letters **60**, 33 (1988).
[7] P. Schild, G. Cottrell, and R. Dendy, Nuclear Fusion **29**, 834 (1989).
[8] G. Cottrell, V. Bhatnagar, O. Da Costa, R. Dendy, J. Jacquinot, K. McClements, D. McCune, M. Nave, P. Smeulders, and D. Start, Nuclear Fusion **33**, 1365 (1993).
[9] K. McClements, C. Hunt, R. Dendy, and G. Cottrell, Physical Review Letters **82**, 2099 (1999).
[10] R. Dendy, K. McClements, C. Lashmore Davies, G. Cottrell, R. Majeski, and S. Cauffman, Nuclear Fusion **35**, 1733 (1995).
[11] S. G. Thatipamula, G. Yun, J. Leem, H. K. Park, K. Kim, T. Akiyama, and S. Lee, Plasma Physics and Controlled Fusion **58**, 065003 (2016).
[12] B. Chapman, R. Dendy, K. McClements, S. Chapman, G. Yun, S. Thatipamula, and M. Kim, Nuclear Fusion **57**, 124004 (2017).
[13] B. Chapman, R. O. Dendy, S. C. Chapman, K. G. McClements, G. S. Yun, S. G. Thatipamula, and M. Kim, Nuclear Fusion **58**, 096027 (2018).
[14] M. Ichimura, H. Higaki, S. Kakimoto, Y. Yamaguchi, K. Nemoto, M. Katano, M. Ishikawa, S. Moriyama, and T. Suzuki, Nuclear Fusion **48**, 035012 (2008).
[15] S. Sumida, K. Shinohara, M. Ichimura, T. Bando, A. Bierwage, and S. Ide, Nuclear Fusion **61**, 116036 (2021).
[16] K. Thome, D. Pace, R. Pinsker, M. Van Zeeland, W. Heidbrink, and M. Austin, Nuclear Fusion **59**, 086011 (2019).
[17] N. A. Crocker, S. X. Tang, K. E. Thome, J. Lestz, E. Belova, A. Zalzali, R. O. Dendy, W. A. Peebles, K. Barada, R. Hong, *et al.*, Nuclear Fusion (2021).
[18] R. Ochoukov, R. Bilato, V. Bobkov, B. Chapman, S. Chapman, R. Dendy, M. Dunne, H. Faugel, M. García-Muñoz, B. Geiger, *et al.*, Nuclear Fusion **59**, 014001 (2018).
[19] R. Ochoukov, K. McClements, R. Bilato, V. Bobkov, B. Chapman, S. Chapman, R. Dendy, M. Dreval, H. Faugel, J.-M. Noterdaeme, *et al.*, Nuclear Fusion **59**, 086032 (2019).
[20] B. Chapman, R. Dendy, S. Chapman, K. McClements, and R. Ochoukov, Plasma Physics and Controlled Fusion **62**, 095022 (2020).
[21] L. Liu, R. Ochoukov, K. McClements, R. Dendy, V. Bobkov, M. Weiland, R. Bilato, H. Faugel, D. Moseev, M. Salewski, *et al.*, Nuclear Fusion **61**, 026004 (2020).
[22] L. Askinazi, A. Belokurov, D. Gin, V. Kornev, S. Lebedev, A. Shevelev, A. Tukachinsky, and N. Zhubr, Nuclear Fusion **58**, 082003 (2018).
[23] L. Askinazi, G. Abdullina, A. Belokurov, V. Kornev, S. Krikunov, S. Lebedev, D. Razumenko, A. Tukachinsky, and N. Zhubr, Technical Physics Letters , 1 (2021).
[24] E. D. Fredrickson, N. Gorelenkov, R. Bell, A. Diallo, B. LeBlanc, M. Podestà, and N. Team, Physics of Plasmas **26**, 032111 (2019).
[25] E. D. Fredrickson, N. N. Gorelenkov, R. E. Bell, A. Diallo, B. P. LeBlanc, J. Lestz, and M. Podesta, Nuclear Fusion **61**, 086007 (2021).
[26] L. Liu, X. Zhang, Y. Zhu, C. Qin, Y. Zhao, S. Yuan, Y. Mao, M. Li, Y. Chen, J. Cheng, *et al.*, Review of Scientific Instruments **90**, 063504 (2019).
[27] K. G. McClements, A. Brisset, B. Chapman, S. C. Chapman, R. O. Dendy, P. Jacquet, V. Kiptily, M. Mantsinen, B. C. Reman, and J. Contributors, Nuclear Fusion **58**, 096020 (2018).
[28] K. Saito, H. Kasahara, T. Seki, R. Kumazawa, T. Mutoh, T. Watanabe, F. Shimpo, G. Nomura, M. Osakabe, M. Ichimura, *et al.*, Fusion Engineering and Design **84**, 1676 (2009).
[29] K. Saito, R. Kumazawa, T. Seki, H. Kasahara, G. Nomura, F. Shimpo, H. Igami, M. Isobe, K. Ogawa, K. Toi, *et al.*, Plasma Science and Technology **15**, 209 (2013).

[30] K. McClements, R. D'Inca, R. Dendy, L. Carbajal, S. Chapman, J. Cook, R. Harvey, W. Heidbrink, and S. Pinches, Nuclear Fusion **55**, 043013 (2015).
[31] R. Dendy and K. McClements, Plasma Physics and controlled fusion **57**, 044002 (2015).
[32] N. N. Gorelenkov, Plasma Physics Reports **42**, 430 (2016).
[33] R. Dendy and K. McClements, Journal of Geophysical Research: Space Physics **98**, 15531 (1993).
[34] K. McClements and R. Dendy, Journal of Geophysical Research: Space Physics **98**, 11689 (1993).
[35] K. G. McClements, R. Dendy, and C. Lashmore-Davies, Journal of Geophysical Research: Space Physics **99**, 23685 (1994).
[36] R. Dendy, Plasma physics and controlled fusion **36**, B163 (1994).
[37] J. Posch, M. Engebretson, C. Olson, S. Thaller, A. Breneman, J. Wygant, S. Boardsen, C. Kletzing, C. Smith, and G. Reeves, Journal of Geophysical Research: Space Physics **120**, 6230 (2015).
[38] V. Rekaa, S. Chapman, and R. Dendy, The Astrophysical Journal **791**, 26 (2014).
[39] B. Chapman, R. Dendy, S. Chapman, L. Holland, S. Irvine, and B. Reman, Plasma Physics and Controlled Fusion **62**, 055003 (2020).
[40] V. Belikov and I. I. Kolesnichenko, Soviet Physics Technical Physics **20**, 1146 (1976).
[41] R. Dendy, C. N. Lashmore Davies, and K. Kam, Physics of Fluids B: Plasma Physics (1989-1993) **4**, 3996 (1992).
[42] R. O. Dendy, C. Lashmore Davies, and K. F. Kam, Physics of Fluids B: Plasma Physics (1989-1993) **5**, 1937 (1993).
[43] R. Dendy, K. McClements, C. Lashmore-Davies, R. Majeski, and S. Cauffman, Physics of Plasmas **1**, 3407 (1994).
[44] R. Dendy, C. Lashmore-Davies, K. McClements, and G. Cottrell, Physics of plasmas **1**, 1918 (1994).
[45] K. G. McClements, R. Dendy, C. Lashmore Davies, G. Cottrell, S. Cauffman, and R. Majeski, Physics of Plasmas **3**, 543 (1996).
[46] T. Fulop, Y. I. Kolesnichenko, M. Lisak, and D. Anderson, Nuclear fusion **37**, 1281 (1997).
[47] T. Fülöp and M. Lisak, Nuclear Fusion **38**, 761 (1998).
[48] T. Fülöp, M. Lisak, Y. I. Kolesnichenko, and D. Anderson, Physics of Plasmas **7**, 1479 (2000).
[49] J. Cook, R. Dendy, and S. Chapman, Plasma Physics and Controlled Fusion **55**, 065003 (2013).
[50] L. Carbajal, R. Dendy, S. Chapman, and J. Cook, Physics of Plasmas **21**, 012106 (2014).
[51] L. Carbajal, R. Dendy, S. Chapman, and J. Cook, Physical Review Letters **118**, 105001 (2017).
[52] L. Carbajal and F. Calderón, Physics of Plasmas **28**, 014505 (2021).
[53] T. Arber, K. Bennett, C. Brady, A. Lawrence-Douglas, M. Ramsay, N. Sircombe, P. Gillies, R. Evans, H. Schmitz, A. Bell, *et al.*, Plasma Physics and Controlled Fusion **57**, 113001 (2015).
[54] J. Cook, R. Dendy, and S. Chapman, Plasma Physics and Controlled Fusion **53**, 074019 (2011).
[55] R. Kubo, Reports on progress in physics **29**, 255 (1966).
[56] J. W. S. Cook, R. O. Dendy, and S. C. Chapman, Phys. Rev. Lett. **118**, 185001 (2017).
[57] A. Kappatou, M. Weiland, R. Bilato, Y. O. Kazakov, R. Dux, V. Bobkov, T. Pütterich, R. M. McDermott, *et al.*, Nuclear Fusion **61**, 036017 (2021).
[58] Y. O. Kazakov, D. Van Eester, R. Dumont, and J. Ongena, Nuclear Fusion **55**, 032001 (2015).
[59] J. Faustin, J. Graves, W. Cooper, S. Lanthaler, L. Villard, D. Pfefferlé, J. Geiger, Y. O. Kazakov, and D. Van Eester, Plasma Physics and Controlled Fusion **59**, 084001 (2017).
[60] V. Bhatnagar, J. Jacquinto, D. Start, and B. Tubbing, Nuclear fusion **33**, 83 (1993).